Research Square

Preprints are preliminary reports that have not undergone peer review.
They should not be considered conclusive, used to inform clinical practice,
or referenced by the media as validated information.

Development and Internal Validation of a Clinical Prediction Model for Trousseau Syndrome in Patients Presenting with Acute Ischemic Stroke

Xianjin Ke
Affiliated Hospital of Jiangsu University
Fan Kong
Jiangsu University
Jing Li
Jiangsu University
Sini Zhu
Jiangsu University
Xian Wu
Affiliated Hospital of Jiangsu University
Guoquan Feng
Affiliated Hospital of Jiangsu University
Deqiang Wang
Affiliated Hospital of Jiangsu University
Kai Niu
Affiliated Hospital of Jiangsu University
Bo Sun
Huaian First People's Hospital
Qiang Wang
qiangwang@ujs.edu.cn

Jiangsu University

Research Article

Keywords: Trousseau syndrome, acute ischemic stroke, prediction model, nomogram, interactive web calculator

Posted Date: November 4th, 2026

DOI: https://doi.org/10.21203/rs.3.rs-11131584/v1

License: This work is licensed under a Creative Commons Attribution 4.0 International License.
Read Full License

Additional Declarations: No competing interests reported.

Abstract

Background

To identify clinical factors associated with Trousseau syndrome presenting as acute ischemic stroke (AIS-TS) and to develop and validate a risk prediction model for AIS-TS, providing a basis for early clinical identification and risk stratification.

Methods

This retrospective study included 51 consecutive patients with AIS-TS who were admitted to the Affiliated Hospital of Jiangsu University between July 2018 and December 2025 as the case group. A control group comprising 204 patients with metastatic solid malignancies without thromboembolic events was selected using 1:4 matching based on admission period. A total of 21 clinical variables were collected, including demographic characteristics, tumor types, and laboratory parameters. Candidate predictors were screened using univariate logistic regression, followed by LASSO regression for dimensionality reduction. A comprehensive scoring approach integrating univariate P-values, random forest variable importance, absolute LASSO coefficients, and odds ratio deviations was applied to determine the final predictive variables. A nomogram was constructed based on the selected variables and internally validated using Bootstrap resampling. Model performance was assessed using the calibration C-index, calibration curves, decision curve analysis (DCA), and clinical impact curves (CIC). An online prediction calculator was developed using the R Shiny platform to facilitate individualized risk assessment.

Results

Univariate logistic regression identified significant differences between groups in age, white blood cell count, platelet count, C-reactive protein (CRP), D-dimer, neutrophil count, carbohydrate antigen 50 (CA50), CA125, CA15-3, CA19-9, and hypertension (all $P < 0.05$). After collinearity assessment and LASSO regression screening, four predictors—D-dimer, platelet count, neutrophil count, and hypertension—were retained. Multivariate logistic regression demonstrated that elevated D-dimer levels (OR = 1.094, 95% CI: 1.039–1.153, $P < 0.001$), increased neutrophil count (OR = 1.123, 95% CI: 1.002–1.259, $P = 0.047$), and hypertension (OR = 2.375, 95% CI: 1.189–4.745, $P = 0.014$) were associated with an increased risk of AIS-TS, whereas lower platelet counts were also associated with higher AIS-TS risk (OR = 0.993, 95% CI: 0.989–0.998, $P = 0.005$). Bootstrap internal validation yielded a calibrated C-index of 0.773 (95% CI: 0.72–0.87), and calibration curves demonstrated good agreement between predicted and observed probabilities. DCA and CIC indicated favorable clinical net benefit across certain threshold probability ranges. An online AIS-TS risk prediction calculator was successfully developed using the Shiny platform.

Conclusion

D-dimer, neutrophil count, platelet count, and hypertension are important factors associated with AIS-TS. The developed prediction model demonstrates good discrimination, calibration, and clinical utility, and may facilitate early identification and risk stratification of patients at increased risk of AIS-TS. The Shiny-based online calculator further improves model accessibility and enables convenient individualized risk assessment for patients with AIS-TS.

Introduction

Malignant tumors represent a substantial global health burden. Thromboembolic events (TEs) are among the most common complications in patients with cancer and are major contributors to cancer-related mortality. In 1865, French physician Armand Trousseau first described the association between malignancy and spontaneous venous thrombosis. Subsequently, the hypercoagulable state associated with cancer and its related thromboembolic complications have been recognized as Trousseau syndrome (TS)[1, 2]. With advances in cancer diagnosis and treatment, improved patient survival has led to an increasing incidence of tumor-associated thrombotic events. Studies have demonstrated that the risk of thrombotic events in patients with cancer is approximately 4–7 times higher than that in the general population without cancer[3].

TS is characterized by clinical heterogeneity and diagnostic challenges, primarily owing to the absence of specific early symptoms, the lack of sensitive and specific biomarkers, and the fact that thrombotic events may precede tumor diagnosis in some patients[4]. Thrombotic events not only delay antitumor therapy, prolong hospitalization, and increase healthcare burden, but also substantially elevate mortality risk[5]. Furthermore, recurrent thromboembolic episodes may lead to chronic pain, limb dysfunction, and neurological impairments in patients with TS, substantially compromising their quality of life[6]. Current treatment strategies for TS remain limited by suboptimal anticoagulant efficacy and increased bleeding risk, necessitating a careful balance between thrombosis prevention and safety[7, 8]. Therefore, early identification of high-risk individuals and the development of effective risk prediction tools are essential for improving patient outcomes.

Research in tumor-associated thrombosis risk assessment has been ongoing for several decades, and the Khorana score remains one of the most widely used clinical tools for predicting the risk of venous thromboembolism (VTE)[9]. In recent years, advances in the understanding of tumor-associated stroke have revealed that a subset of cryptogenic strokes may be associated with occult malignancies. Consequently, the Trousseau score was developed based on clinical characteristics and laboratory markers to estimate the likelihood of a tumor-related etiology in patients with cryptogenic stroke [10]. However, effective risk prediction models for patients presenting with acute ischemic stroke (AIS) as a manifestation of TS are still lacking.

In recent years, machine learning and statistical learning approaches have been increasingly applied to the development of clinical prediction models. The least absolute shrinkage and selection operator (LASSO) regression effectively addresses multicollinearity and facilitates high-dimensional variable selection[11]. However, in settings with limited sample sizes and variables exhibiting strong effects,

LASSO may preferentially retain only a single dominant predictor, potentially resulting in the loss of clinically relevant information. Therefore, integrating multiple variable importance assessment methods for comprehensive feature selection may enhance model stability and improve clinical interpretability[12, 13].

This study systematically analyzed the clinical characteristics and associated factors of TS patients presenting with AIS (AIS-TS) patients using single-center clinical data and employed a multidimensional variable selection strategy to develop and validate an AIS-TS risk prediction model, aiming to provide evidence for the early identification and individualized risk assessment of TS in patients with AIS.

Materials and Methods

Study design and participants

This was a single-center, retrospective matched case-control study. A total of 51 consecutive patients with TS presenting as AIS were enrolled from the Affiliated Hospital of Jiangsu University between July 2018 and December 2025 as the case group. The control group comprised 204 patients with metastatic solid malignancies hospitalized during the same period, frequency-matched to the case group at a 1:4 ratio according to tumor type distribution. None of the control patients had evidence of thromboembolic events. The study was approved by the Ethics Committee of the Affiliated Hospital of Jiangsu University (approval number: KY2021K1005).

The inclusion criteria for the case group were as follows: (1) age ≥ 18 years; (2) confirmed diagnosis of solid malignancy based on pathological and/or imaging findings (excluding hematologic malignancies and primary intracranial tumors); (3) diagnosis of AIS according to established criteria, with TS diagnosed based on clinical presentation, imaging characteristics, and laboratory findings after systematic exclusion of other known thrombotic mechanisms; and (4) availability of complete clinical and laboratory data.

The inclusion criteria for the control group were as follows: (1) age ≥ 18 years; (2) presence of metastatic solid malignancies hospitalized during the same period, with histopathological types identical or similar to those of the case group; (3) absence of AIS or other thromboembolic events; and (4) availability of complete clinical data.

The exclusion criteria were as follows: (1) presence of known high-risk cardioembolic conditions, including atrial fibrillation, previous cardiac valve replacement, or infective endocarditis; (2) definite large-artery atherosclerotic stroke (e.g., carotid stenosis ≥ 50%) or small-vessel occlusive cerebral infarction; (3) cerebral embolism attributable to other identifiable etiologies, including eosinophilia, systemic vasculitis, or infection-related thrombosis; (4) hematologic malignancies or primary intracranial tumors; and (5) missing key clinical variables.

Data collection

Baseline clinical data were obtained from the hospital's electronic medical record system, including sex, age, smoking history, alcohol consumption history, and medical history of hypertension, diabetes, coronary heart disease, and prior stroke, as well as tumor type and laboratory test results. Laboratory parameters included D-dimer, C-reactive protein (CRP), platelet count (PLT), mean platelet volume (MPV), white blood cell count (WBC), neutrophil count (NEUT), carcinoembryonic antigen (CEA), carbohydrate antigen 50 (CA50), carbohydrate antigen 125 (CA125), carbohydrate antigen 15 − 3 (CA15-3), carbohydrate antigen 19 − 9 (CA19-9), and neuron-specific enolase (NSE).

Statistical analysis

Statistical analyses were performed using SPSS 25.0 and R 4.2.1 software. Continuous variables with a normal distribution were presented as mean ± standard deviation ($\bar{x} \pm s$) and compared between groups using independent-samples t-tests. Continuous variables with non-normal distributions were expressed as median (interquartile range) and analyzed using the Mann–Whitney U test. Categorical variables were presented as counts (percentages) and compared using the χ^2 test or Fisher's exact test. A two-sided P value < 0.05 was considered statistically significant.

First, univariate Logistic regression analysis was performed for candidate variables, and variables with statistically significant differences were selected for further analysis. Multicollinearity was assessed using the variance inflation factor (VIF), and variables with VIF > 5 were screened or excluded based on statistical significance and clinical relevance[14]. LASSO regression was subsequently applied for variable selection and dimensionality reduction, with the optimal penalty parameter λ determined by cross-validation to identify potential predictors. To minimize the risk of omitting clinically relevant variables associated with single-method selection, a comprehensive variable assessment integrating univariate P-values, random forest variable importance, the absolute values of LASSO regression coefficients, and deviations in odds ratios (ORs) was performed to determine the final model variables. A multivariable Logistic regression model was then constructed to predict the risk of AIS-TS, and the ORs, 95% confidence intervals (CIs), and P-values were calculated for each predictor. Internal validation was conducted using the bootstrap method with 1,000 resamples to obtain the optimism-corrected C-index and generate calibration curves for evaluating model stability. Decision curve analysis (DCA) was performed to assess the clinical net benefit of the model, while clinical impact curves (CICs) were used to evaluate its ability to identify high-risk patients across different risk thresholds. Finally, an online AIS-TS risk prediction calculator was developed using the Shiny package in R and the RStudio platform to facilitate visualized application of the model.

Results

Imaging characteristics of typical AIS-TS patients

All patients underwent brain magnetic resonance imaging (MRI) examination. Figure 1 illustrates the imaging findings of a typical AIS-TS patient. Diffusion-weighted imaging (DWI) demonstrated multiple scattered acute ischemic lesions involving both anterior and posterior circulation territories, consistent

with a multifocal embolic pattern of cerebral infarction. Computed tomography angiography (CTA) of the intracranial and extracranial vessels revealed no significant stenosis or occlusion.

Comparison of clinical baseline characteristics between the two groups

No statistically significant differences were observed between the case and control groups in terms of sex, smoking, alcohol, or other baseline characteristics (all $P > 0.05$). However, significant differences were found in age and history of hypertension between the two groups (both $P < 0.05$). Based on the primary tumor origin, patients were categorized into three groups: digestive system tumors, respiratory system tumors, and reproductive system tumors. The distribution of tumor types did not differ significantly between the two groups ($P > 0.05$).

Laboratory examinations showed that the levels of D-dimer, WBC, NEUT, CRP, CA50, CA125, CA19-9, CA15-3, and NSE were significantly higher in the case group than in the control group, whereas PLT was significantly lower in the case group (all $P < 0.05$) (Table 1).

Table 1
Comparison of clinical Baseline characteristics between the two groups

Variable	Total (N = 255)	Patients (N = 51)	Controls (N = 204)	*Z* value	*P* value
Continuous variables					
Age (years)	67(60,75)	70(65,76)	66(58.25,74)	2.787	0.005
WBC ($\times 10^9$/L)	6.40(4.90,8)	7.60(6,8.90)	6.10(4.70,7.75)	3.629	< 0.001
NEUT ($\times 10^9$/L)	4.30(3,5.90)	5.60(4.20,6.70)	4(2.90,5.70)	3.708	< 0.001
PLT ($\times 10^9$/L)	199(148,260)	162(104,219)	205(155.75,266.25)	3.162	0.002
MCV (fL)	10.60(9.70,11.60)	10.40(9.50,11.50)	10.60(9.80,11.60)	1.132	0.258
CRP (mg/L)	6.90(1.60,23.90)	19.80(3.10,59.50)	5.70(1.03,18.70)	4.084	< 0.001
D-dimer (mg/L)	1.26(0.51,3.88)	5.76(2.37,9.12)	0.93(0.43,2.24)	7.268	< 0.001
CEA (ng/mL)	8.38(3.31, 34.27)	14.73(3.96, 50.09)	8.10(3.23, 26.04)	1.571	0.116
CA-50 (U/mL)	16(5.60,122.59)	54.28(18.47,432.68)	12.185(4.93,105.58)	3.703	< 0.001
CA-125 (U/mL)	45.30(18.60,145.40)	92.90(33.90,326.70)	38.40(16.35,111.63)	3.363	< 0.001
CA 19 – 9 (U/mL)	25.54(8.15,288.25)	79.73(16.38,1000)	21.49(7.47,198.76)	2.961	0.003
CA 15 – 3 (U/mL)	15.22(9.06,38.96)	38.96(16.20,83.27)	13.22(8.67,29.15)	4.449	< 0.001
NSE (ng/mL)	4.30(3.30,6.80)	6.7(4.50,10.30)	4.10(3.10,5.68)	4.453	< 0.001
Categorical variables				χ^2 value	*P* value
Sex (n%)				0.004	0.948
Male	159(62.35)	32(62.75)	127(62.25)	-	-
Female	96(37.65)	19(37.25)	77(37.75)	-	-

WBC: White blood cell; NEUT: Neutrophils; PLT: Platelets; MCV: Mean corpuscular volume; CRP: C-reactive protein; CEA: carcinoembryonic antigen; CA-50: carbohydrate antigen; CA-125: carbohydrate antigen 125; CA19-9: carbohydrate antigen 19 – 9; CA15-3: carbohydrate antigen 15 – 3; NSE: Neuron-specific enolase

Variable	Total (N = 255)	Patients (N = 51)	Controls (N = 204)	*Z* value	*P* value
Tumor type (n%)	-	-	-	0.244	0.885
Respiratory system tumor	78(30.59)	15(29.41)	63(30.88)	-	-
Digestive system tumor	147(57.65)	29(56.86)	118(57.84)	-	-
Reproductive system tumor	30(11.76)	7(13.73)	23(11.27)	-	-
Smoking (n%)	69(27.06)	14(27.45)	55(26.96)	0.005	0.944
Alcohol (n%)	36(14.12)	7(13.73)	29(14.22)	0.008	0.928
Coronary heart disease (n%)	18(7.06)	1(1.96)	17(8.33)	-	0.136
Stroke (n%)	23(9.02)	7(13.73)	16(7.84)	-	0.183
Hypertension (n%)	111(43.53)	30(58.82)	81(39.71)	6.066	0.014
Diabetes mellitus (n%)	40(15.69)	7(13.73)	33(16.18)	0.185	0.667

WBC: White blood cell; NEUT: Neutrophils; PLT: Platelets; MCV: Mean corpuscular volume; CRP: C-reactive protein; CEA: carcinoembryonic antigen; CA-50: carbohydrate antigen; CA-125: carbohydrate antigen 125; CA19-9: carbohydrate antigen 19 − 9; CA15-3: carbohydrate antigen 15 − 3; NSE: Neuron-specific enolase

Univariate and multivariate Logistic regression analysis to identify predictive variables

Univariate logistic regression analysis identified 11 variables significantly associated with the occurrence of AIS-TS, including age, hypertension, D-dimer, WBC, NEUT, PLT, CRP, CA50, CA125, CA19-9, and CA15-3 (all $P < 0.05$) (Table 2). After evaluating multicollinearity among candidate variables, variable selection was performed based on statistical significance and clinical relevance (Supplementary Material). Ultimately, four variables—D-dimer, NEUT, PLT, and hypertension—were included in the multivariable logistic regression model.

The results demonstrated that elevated D-dimer levels (OR = 1.094, 95% CI: 1.039–1.153, $P < 0.001$), increased NEUT levels (OR = 1.123, 95% CI: 1.002–1.259, $P = 0.047$), and hypertension (OR = 2.375, 95% CI:

1.189–4.745, P = 0.014) were independently associated with an increased risk of AIS-TS, whereas higher PLT levels were associated with a reduced risk of AIS-TS (OR = 0.993, 95% CI: 0.989–0.998, P = 0.005) (Table 2). The Hosmer–Lemeshow goodness-of-fit test showed $\chi^2 = 13.557$ (P = 0.094), indicating good model calibration. The Nagelkerke R^2 value was 0.238, and the overall classification accuracy of the model was 81.2%.

Table 2
Univariate and multivariate Logistic regression analysis for identifying predictors of AIS-TS

Variable	Univariate			Multivariate		
	OR	95%CI	P value	OR	95%CI	P value
Continuous variables						
Age	1.047	(1.013,1.081)	0.006			
WBC	1.121	(1.026,1.225)	0.012			
NEUT	1.141	(1.036,1.257)	0.007	1.123	(1.002,1.259)	0.047
PLT	0.993	(0.989,0.998)	0.002	0.993	(0.989,0.998)	0.005
MCV	0.927	(0.750,1.146)	0.484			
CRP	1.015	(1.006,1.024)	0.001			
D-dimer	1.119	(1.064,1.176)	< 0.001	1.094	(1.039,1.153)	< 0.001
CEA	1.000	(0.998,1.002)	0.951			
CA-50	1.003	(1.001,1.004)	0.002			
CA-125	1.001	(1.000,1.002)	0.018			
CA 19 – 9	1.001	(1.000,1.002)	0.010			
CA 15 – 3	1.004	(1.001,1.007)	0.017			
NSE	1.000	(0.991,1.010)	0.955			
Categorical variables						
Sex	0.979	(0.519,1.847)	0.948			
Tumor type						
Digestive system vs. Respiratory system	1.032	(0.515,2.067)	0.929			
Reproductive system vs. Respiratory system	1.278	(0.463,3.532)	0.636			
Smoking history	1.025	(0.515,2.040)	0.944			
Alcohol consumption	0.960	(0.395,2.336)	0.928			

WBC: White blood cell; NEUT: Neutrophils; PLT: Platelets; MCV: Mean corpuscular volume; CRP: C-reactive protein; CEA: carcinoembryonic antigen; CA-50: carbohydrate antigen; CA-125: carbohydrate antigen 125; CA19-9: carbohydrate antigen 19 – 9; CA15-3: carbohydrate antigen 15 – 3; NSE: Neuron-specific enolase

Variable	Univariate			Multivariate		
	OR	95%CI	P value	OR	95%CI	P value
Coronary heart disease	0.220	(0.029,1.693)	0.146			
Stroke	1.869	(0.725,4.819)	0.195			
Hypertension	2.169	(1.162,4.050)	0.015	2.375	(1.189,4.745)	0.014
Diabetes mellitus	0.824	(0.342,1.988)	0.667			

WBC: White blood cell; NEUT: Neutrophils; PLT: Platelets; MCV: Mean corpuscular volume; CRP: C-reactive protein; CEA: carcinoembryonic antigen; CA-50: carbohydrate antigen; CA-125: carbohydrate antigen 125; CA19-9: carbohydrate antigen 19 – 9; CA15-3: carbohydrate antigen 15 – 3; NSE: Neuron-specific enolase

Variable selection and reduction using LASSO regression

To identify candidate predictors for model development, LASSO regression with 10-fold cross-validation was performed for variable selection and dimensionality reduction. The cross-validation curve demonstrated the relationship between the penalty parameter (λ) and model deviance, with λ_min representing the value of λ associated with the minimum cross-validation error and λ_1SE representing the largest λ value within one standard error of the minimum cross-validation error. In this study, the λ_1SE criterion was adopted to construct a parsimonious predictive model and reduce the risk of overfitting (Fig. 2A). The LASSO coefficient trajectory plot showed that, as the penalty strength increased, the regression coefficients of most variables gradually shrank toward zero (Fig. 2B). At the λ_1SE threshold, LASSO regression automatically identified one predictor with a non-zero coefficient. To balance clinical relevance and the coverage of potential predictors, three additional variables were further incorporated based on their overall variable importance rankings and clinical significance (Supplementary Materials). Ultimately, four candidate predictors were selected and entered into multivariable analysis for predictive model development.

Construction of the AIS-TS prediction model, internal validation, and evaluation of clinical utility

A risk prediction nomogram for AIS-TS was developed based on four predictors: D-dimer, NEUT, PLT, and hypertension (Fig. 3). The regression coefficients of each predictor were transformed into corresponding point values, with a total score ranging from 0 to 200. The individual risk of AIS-TS was estimated using the probability scale corresponding to the total score.

Internal validation was performed using the bootstrap method with 1,000 resamples. The original C-index of the model was 0.786, which slightly decreased to 0.773 (95% CI: 0.72–0.87) after bootstrap correction, indicating good discriminatory performance. The calibration curve demonstrated good agreement

between predicted and observed probabilities, with a mean absolute error of 0.04 (Fig. 4). DCA showed that, within a specific range of threshold probabilities, the prediction model provided greater clinical net benefit than the “treat-all” or “treat-none” strategies. The CIC further indicated that the model effectively identified patients at high risk of AIS-TS (Fig. 5).

Online risk prediction tool development

Based on the final multivariable Logistic regression model, an online AIS-TS risk prediction calculator was developed using the Shiny package in R (Fig. 6). The tool incorporates four predictive variables—D-dimer, NEUT, PLT, and hypertension—to enable individualized risk estimation and visualized presentation of AIS-TS probability. Users can access the tool through a web browser at the following URL:https://lijing123.shinyapps.io/TrousseauSyndromeRiskCalculator

Discussion

This study developed and internally validated a risk prediction model for AIS-TS using four routinely available variables: D-dimer, neutrophil count, platelet count, and hypertension. The model demonstrated moderate-to-good discrimination (corrected C-index 0.773), satisfactory calibration (mean absolute error 0.04), and favorable clinical net benefit by DCA and CIC. An online Shiny calculator was further constructed to facilitate individualized risk estimation. These findings extend our previous work on AIS-TS, in which D-dimer and systemic immune-inflammation index (SII) were associated with diagnosis and prognosis [15, 16], by providing a practical multivariable tool for early risk stratification.

Among the four predictors, D-dimer was the only variable consistently retained by LASSO and remained independently associated with AIS-TS in multivariable analysis (OR = 1.094, 95% CI: 1.039–1.153, P < 0.001). This supports the central role of coagulation activation and fibrin degradation in AIS-TS. In our previous study, elevated D-dimer was also associated with poor survival in patients with AIS-TS[15]. Taken together, D-dimer may serve not only as a predictive marker but also as a candidate for dynamic monitoring of thrombotic burden and treatment response.

Neutrophil count was independently associated with AIS-TS (OR = 1.123, 95% CI: 1.002–1.259, P = 0.047). This finding is consistent with our prior observation that SII, an inflammation-based composite index, predicted TS initially presenting with AIS[16]. It supports the concept that neutrophil-mediated inflammation contributes to the prothrombotic state in TS, possibly through cytokine release and neutrophil extracellular traps (NETs) formation[17–20]. However, the modest OR and wide confidence interval indicate that neutrophil count alone is insufficient; its inclusion mainly improves risk estimation together with other variables.

Reduced platelet count was associated with increased AIS-TS risk (OR = 0.993, 95% CI: 0.989–0.998, P = 0.005). This inverse association is clinically plausible in TS: widespread microthrombus formation and platelet-rich thrombus consumption may lead to peripheral platelet depletion, especially in mucin-secreting adenocarcinoma [2, 21]. This result also aligns with prior scoring studies in cancer-associated

stroke[10]. Therefore, thrombocytopenia in patients with malignancy and AIS should not be simply ignored; it may reflect an ongoing consumptive hypercoagulable state and should raise suspicion for AIS-TS.

Hypertension was independently associated with AIS-TS (OR = 2.375, 95% CI: 1.189–4.745, P = 0.014). Because common stroke etiologies such as large-artery atherosclerosis and small-vessel disease were rigorously excluded, this association suggests that hypertension may contribute to AIS-TS beyond its role as a conventional cerebrovascular risk factor. Mechanistically, hypertension can promote endothelial dysfunction, oxidative stress, and coagulation activation, thereby amplifying the tumor-associated prothrombotic phenotype[22–24]. Clinically, a history of hypertension should be considered when assessing AIS-TS risk in cancer patients.

The nomogram incorporating these four variables provides an accessible tool for individualized risk estimation. Internal validation showed a corrected C-index of 0.773 (95% CI: 0.72–0.87), with good agreement between predicted and observed probabilities. DCA and CIC indicated net benefit across a range of threshold probabilities, and the Shiny calculator further improves bedside applicability. These features make the model potentially useful for early identification of AIS-TS in patients presenting with AIS and known or suspected malignancy.

Several limitations should be acknowledged. This was a single-center retrospective study with a relatively small sample size, and the model was not externally validated. The model is also static, based on admission variables, whereas thrombotic risk may change over time. Future multicenter studies with larger cohorts and dynamic prediction approaches are needed to confirm and refine the model.

In conclusion, this study identified D-dimer, neutrophil count, platelet count, and hypertension as independent factors for AIS-TS and developed a practical prediction model with good discrimination, calibration, and clinical utility. The model extends our previous AIS-TS research and provides a promising tool for early risk stratification, pending external validation.

Declarations

Ethics approval and consent to participate

This study was conducted in accordance with the ethical principles of the Declaration of Helsinki and was approved by the Ethics Committee of the Affiliated Hospital of Jiangsu University (approval No. KY2021K1005). Written informed consent for participation was obtained from the patients or, where applicable, from their legally authorized family members on their behalf.

Consent for publication

Not applicable.

Competing interests

The authors declare no competing interests.

Funding

This work was supported in part by the “Beigu Talent” Cultivation Program of the Affiliated Hospital of Jiangsu University and the Zhenjiang Social Development Project (Grant No. SH2025065).

Author Contribution

Xianjin Ke, Fan Kong, Jing Li, Sini Zhu, Xian Wu, Guoquan Feng, Deqiang Wang and Kai Niu contributed to the acquisition of patient data. Xianjin Ke, Fan Kong and Jing Li were responsible for drafting and critically revising the manuscript. Xian Wu, Deqiang Wang and Guoquan Feng contributed to the preparation of the figures and tables. Qiang Wang and Bo Sun provided final approval of the version to be published. All authors made substantial contributions to the conception and design of the study, or to the acquisition, analysis, and interpretation of data, and all authors reviewed and approved the final manuscript.

Acknowledgement

We sincerely thank all participants for their generous contribution of data to this study.

Data Availability

The data supporting the findings of this study are available from the corresponding author, Bo Sun, or the first author, Xianjin Ke, upon reasonable request.

References

1. Khorana AA, Francis CW, Culakova E, Kuderer NM, Lyman GH. Thromboembolism is a leading cause of death in cancer patients receiving outpatient chemotherapy. J Thromb Haemost. 2007;5:632–4. https://doi.org/10.1111/j.1538-7836.2007.02374.x.
2. Varki A. Trousseau's syndrome: multiple definitions and multiple mechanisms. Blood. 2007;110:1723–9. https://doi.org/10.1182/blood-2006-10-053736.
3. Mukai M, Oka T. Mechanism and management of cancer-associated thrombosis. J Cardiol. 2018;72:89–93. https://doi.org/10.1016/j.jjcc.2018.02.011.
4. Ren R, Yan H, Gui Y, Zhao J, Wang H, Ji D, et al. Clinical Features of Trousseau Syndrome With Cerebral Infarction as the Initial Manifestation. Neurologist. 2020;25:117–21. https://doi.org/10.1097/NRL.0000000000000275.

5. Streiff MB, Holmstrom B, Angelini D, Ashrani A, Buckner T, Diep R, et al. Cancer-Associated Venous Thromboembolic Disease, Version 2.2024, NCCN Clinical Practice Guidelines in Oncology. J Natl Compr Canc Netw. 2024;22:483–506. https://doi.org/10.6004/jnccn.2024.0046.
6. Liu H, Jiang M, Wu N, Liu Q, Fan X. A case of Trousseau syndrome: Screening, detection and complication. Open Life Sci. 2024;19:20220824. https://doi.org/10.1515/biol-2022-0824.
7. Kang W, Huang C, Yan VKC, Wei Y, Shami JJP, Li STH, et al. Effectiveness and safety of continuous low-molecular-weight heparin versus switching to direct oral anticoagulants in cancer-associated venous thrombosis. Nat Commun. 2024;15:5657. https://doi.org/10.1038/s41467-024-50037-1.
8. Zwicker JI. Trousseau syndrome: management of refractory VTE. Hematology Am Soc Hematol Educ Program. 2024; 2024, 253–258. https://doi.org/10.1182/hematology.2024000552
9. Khorana AA, Kuderer NM, Culakova E, Lyman GH, Francis CW. Development and validation of a predictive model for chemotherapy-associated thrombosis. Blood. 2008;111:4902–7. https://doi.org/10.1182/blood-2007-10-116327.
10. Hasegawa Y, Setoguchi T, Sakaida T, Iuchi T. Utility of a scoring system for differentiating cancer-associated stroke from cryptogenic stroke in patients with cancer. Neurol Sci. 2020;41:1245–50. https://doi.org/10.1007/s10072-019-04231-5.
11. Xi LJ, Guo ZY, Yang XK, Ping ZG. [Application of LASSO and its extended method in variable selection of regression analysis]. Zhonghua Yu Fang Yi Xue Za Zhi. 2023;57:107–11. https://doi.org/10.3760/cma.j.cn112150-20220117-00063.
12. Sanchez-Pinto LN, Venable LR, Fahrenbach J, Churpek MM. Comparison of variable selection methods for clinical predictive modeling. Int J Med Inf. 2018;116:10–7. https://doi.org/10.1016/j.ijmedinf.2018.05.006.
13. Bagherzadeh-Khiabani F, Ramezankhani A, Azizi F, Hadaegh F, Steyerberg EW, Khalili D. A tutorial on variable selection for clinical prediction models: feature selection methods in data mining could improve the results. J Clin Epidemiol. 2016;71:76–85. https://doi.org/10.1016/j.jclinepi.2015.10.002.
14. Bollmann S, Groll A, Havranek MM. Accounting for clustering in automated variable selection using hospital data: a comparison of different LASSO approaches. BMC Med Res Methodol. 2023;23:280. https://doi.org/10.1186/s12874-023-02081-6.
15. Ke X, Wu X, Feng G, Wang D, Niu K, Zhu Y, et al. Analysis of Prognostic Factors for Survival in Patients with Trousseau Syndrome Initially Presenting with Acute Ischemic Stroke. Cerebrovasc Dis Extra. 2025;1–11. https://doi.org/10.1159/000548109.
16. Ke X, Feng WX, Wang G, Niu D, Zhu K. Evaluation of the systemic immune-inflammation index in the diagnosis of Trousseau syndrome initially presenting with acute ischemic stroke. Eur J Med Res. 2026;638. https://doi.org/10.1186/s40001-026-04228-9.
17. Alexander ET, Gilmour SK. Immunomodulatory role of thrombin in cancer progression. Mol Carcinog. 2022;61:527–36. https://doi.org/10.1002/mc.23398.
18. Pantazi D, Alivertis D, Tselepis AD. Underlying Mechanisms of Thrombosis Associated with Cancer and Anticancer Therapies. Curr Treat Options Oncol. 2024;25:897–913.

https://doi.org/10.1007/s11864-024-01210-7.

19. Chen J, Xu Y, Yu F, Ma Z, Yu J, Zhang X. NETs: an extracellular DNA network structure with implication for cardiovascular disease and cancer. Hypertens Res. 2024;47:1260–72. https://doi.org/10.1038/s41440-023-01574-7.
20. Paramo JA. Neutrophils as instigators of thrombosis: Beyond antimicrobial protection. Rev Clin Esp. 2020;220:583–6. https://doi.org/10.1016/j.rce.2019.11.013.
21. Sack GH Jr., Levin J, Bell WR. Trousseau's syndrome and other manifestations of chronic disseminated coagulopathy in patients with neoplasms: clinical, pathophysiologic, and therapeutic features. Med (Baltim). 1977;56:1–37.
22. Fadl YY, Zareba W, Moss AJ, Marder VJ, Sparks CS, Miller Watelet LF, et al. History of hypertension and enhanced thrombogenic activity in postinfarction patients. Hypertension. 2003;41:943–9. https://doi.org/10.1161/01.HYP.0000061120.23237.D9.
23. Correa HL, Deus LA, Nascimento DDC, Rolnick N, Neves RVP, Reis AL, et al. Concerns about the application of resistance exercise with blood-flow restriction and thrombosis risk in hemodialysis patients. J Sport Health Sci. 2024;13:548–58. https://doi.org/10.1016/j.jshs.2024.02.006.
24. Wang R. Roles of Hydrogen Sulfide in Hypertension Development and Its Complications: What, So What, Now What. Hypertension. 2023;80:936–44. https://doi.org/10.1161/HYPERTENSIONAHA.122.19456.

Figures

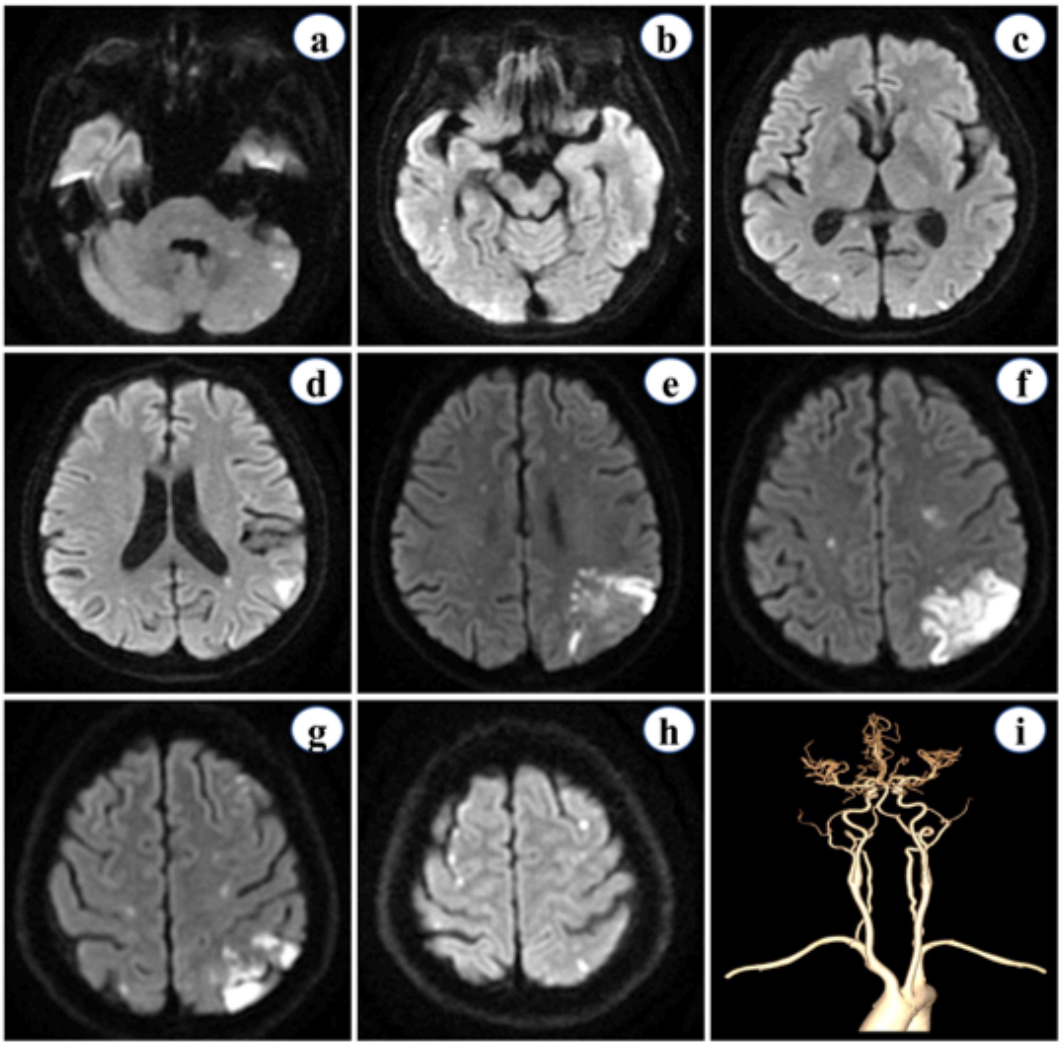


Figure 1

illustrates brain MRI findings in a representative patient diagnosed with Trousseau syndrome. DWI images demonstrate multiple acute ischemic lesions—characterized by hyperintense signals—distributed across both anterior and posterior cerebral circulations, consistent with embolic infarction□a-h□. Image i presents contrast-enhanced CTA, which reveals no hemodynamically significant stenosis or occlusion of major intracranial arteries.

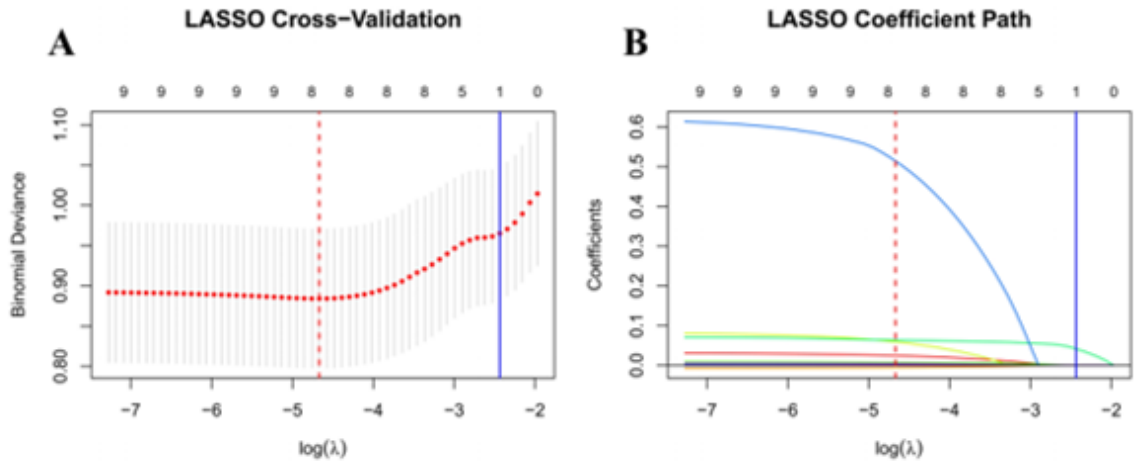


Figure 2

Variable selection using LASSO regression. (A) Cross-validation curve for selecting the optimal penalty parameter (λ). The red dashed line indicates λ min, and the blue solid line represents λ_1SE. (B) LASSO coefficient profile plot showing changes in variable coefficients with increasing log(λ). Each curve represents an individual predictor. At λ_1SE, only one predictor (blue curve) retained a non-zero coefficient.

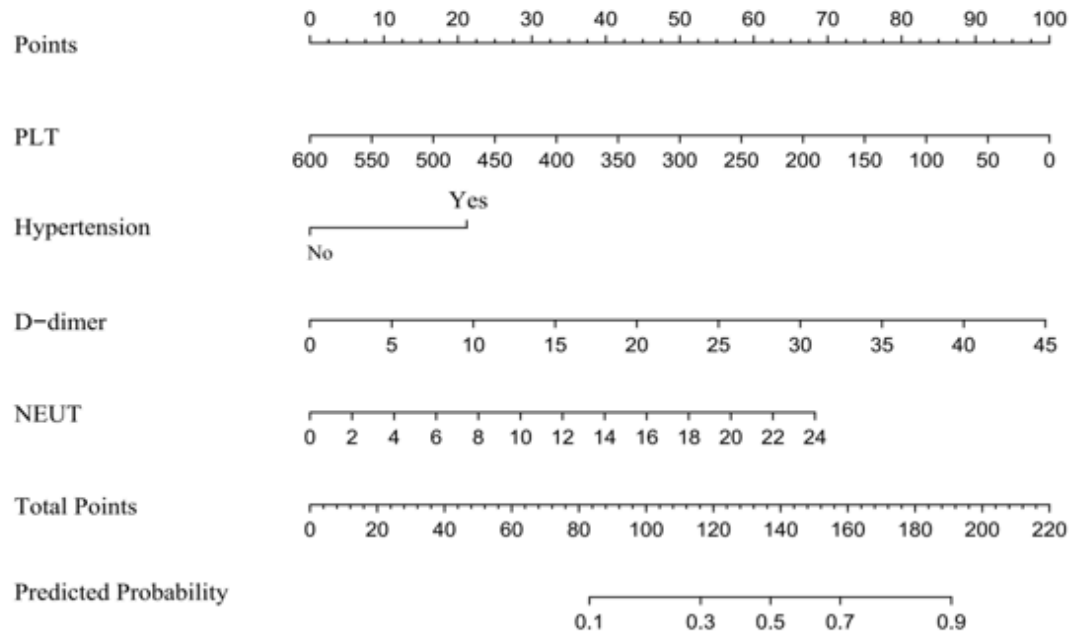


Figure 3

AIS-TS prediction Nomogram. To use this nomogram, identify the patient-specific value for each covariate on its corresponding axis, draw a vertical line upward to the “Points” scale to assign the respective point score, sum all individual scores to obtain the total points, locate this sum on the “Total Points” axis, and

finally draw a vertical line downward to the “Predicted Probability of AIS-TS” axis to read the estimated probability. PLT: Platelets; NEUT: Neutrophils

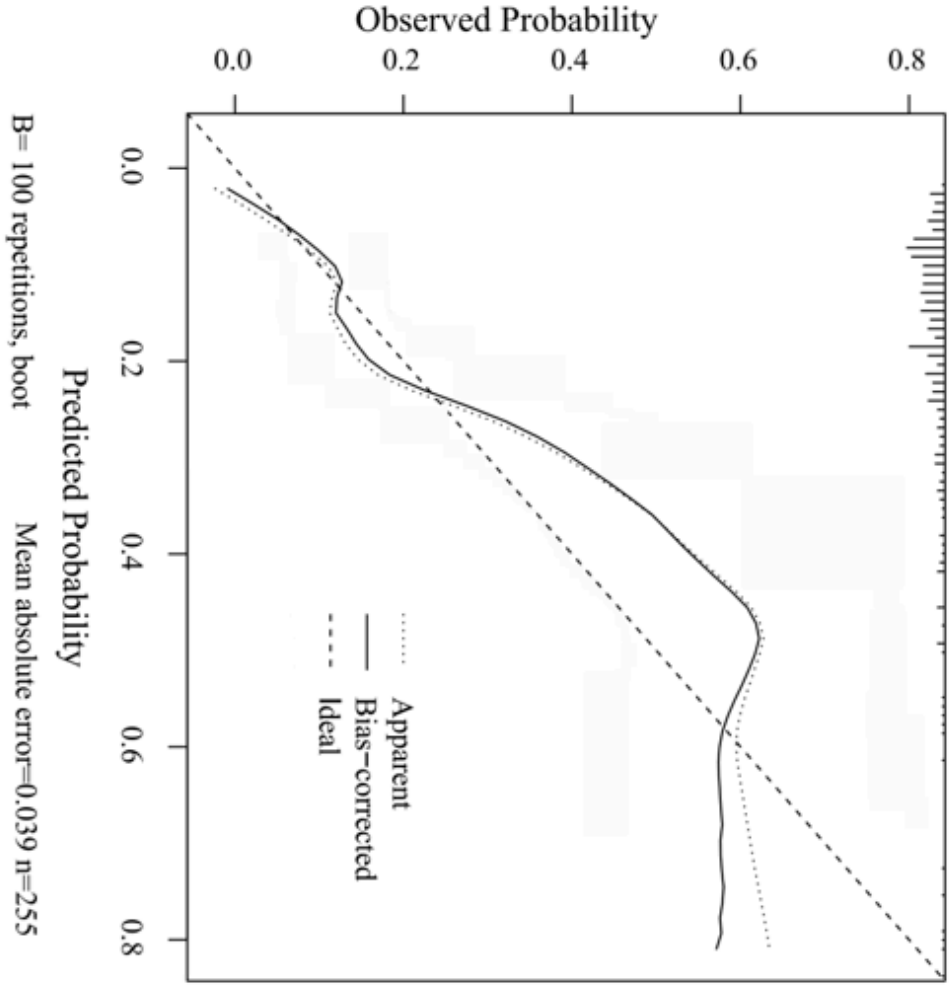


Figure 4

Internal validation of the Nomogram these calibration curves depict the relationship between predicted probability (x-axis) and observed event frequency (y-axis), with the diagonal line representing perfect calibration.

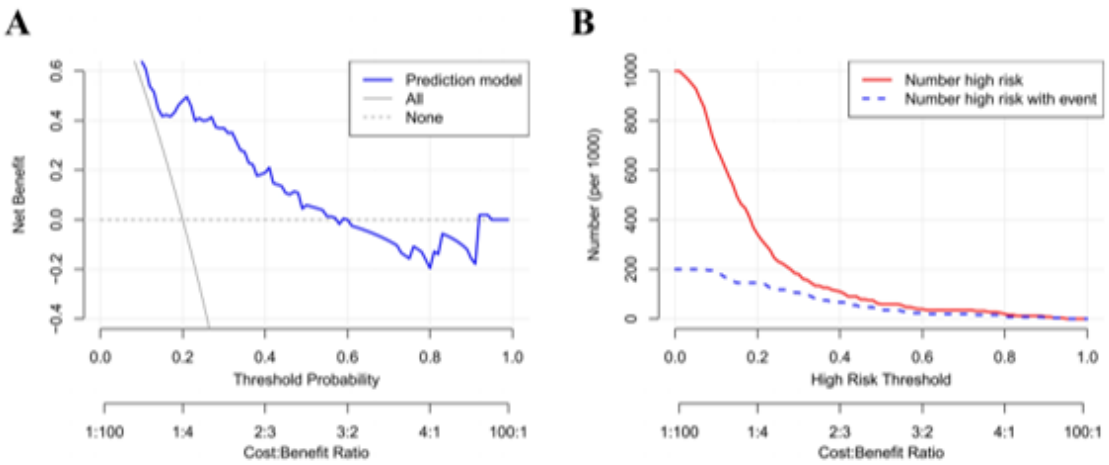


Figure 5

Clinical utility assessment using decision curve analysis (DCA) and clinical impact curve (CIC). A. DCA of the nomogram. The y-axis represents net benefit, and the x-axis is the threshold probability considered by clinicians for diagnosis. B. CIC of the nomogram. The red curve ("Number of high-risk patients") shows the number of patients per 1,000 who would be classified as high risk across a continuum of probability thresholds under clinical application of the nomogram. The blue curve ("Number of AIS-TS events among high-risk patients") displays the corresponding number of patients who subsequently experienced the AIS-TS event.

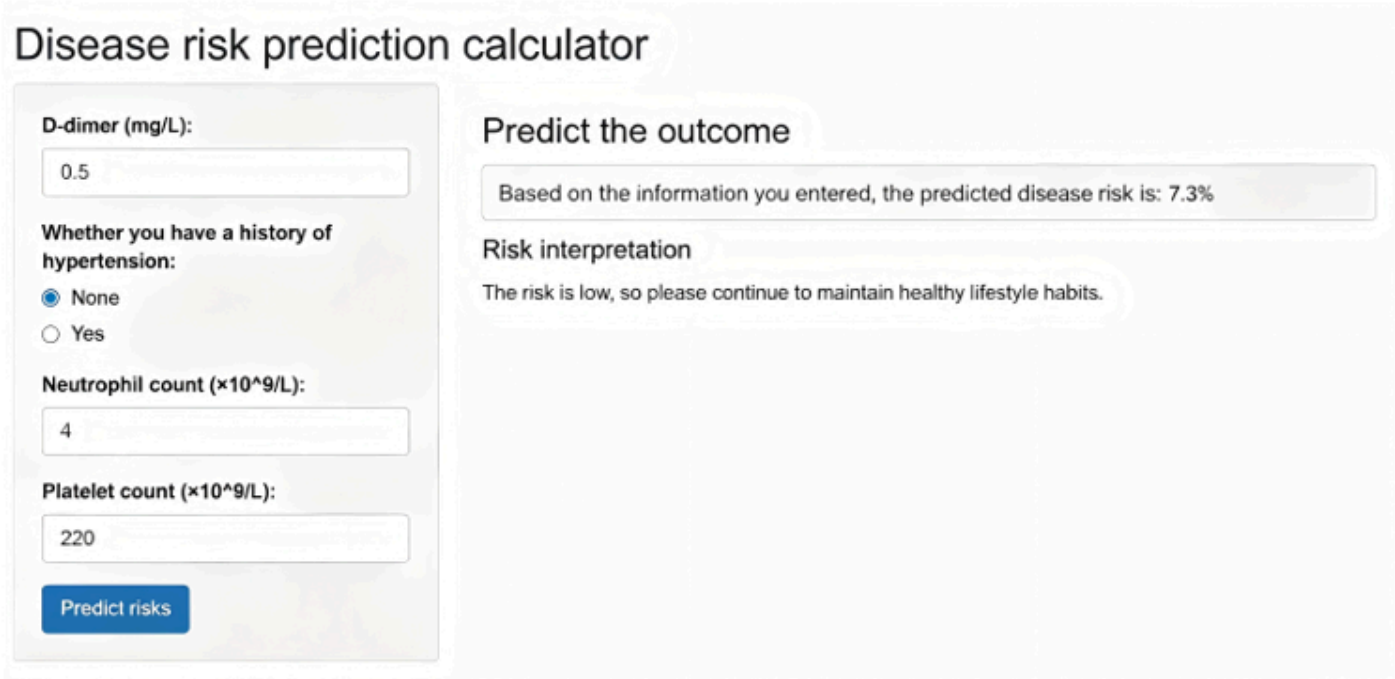


Figure 6

Developing a clinical prediction AIS-TS web calculator using the Shiny package in R and provides an online web calculator link

Supplementary Files

This is a list of supplementary files associated with this preprint. Click to download.

- 5TS4Tabs.docx
- 5SupplementaryMaterial.docx